

# **Seasonal Dynamics of Epiphytic Microbial Communities on Marine Macrophyte Surfaces**

Marino Korlević<sup>1\*</sup>, Marsej Markovski<sup>1</sup>, Zihao Zhao<sup>2</sup>, Gerhard J. Herndl<sup>2,3</sup>, Mirjana Najdek<sup>1</sup>

\*To whom correspondence should be addressed: marino.korlevic@irb.hr

1. Center for Marine Research, Ruđer Bošković Institute, Croatia
2. Department of Functional and Evolutionary Ecology, University of Vienna, Austria
3. Department of Marine Microbiology and Biogeochemistry, Royal Netherlands Institute for Sea Research, Utrecht University, The Netherlands

## 1 Abstract

2 Surfaces of marine macrophytes (seagrasses and macroalgae) are inhabited by diverse  
3 microbial communities. Most studies focusing on macrophyte epiphytic communities did not  
4 take into account temporal changes or applied low sampling frequency approaches. Illumina  
5 sequencing of the V4 16S rRNA region was performed to determine the seasonal dynamics  
6 of epiphytic communities sampled from the surfaces of the seagrass *Cymodocea nodosa* and  
7 invasive macroalga *Caulerpa cylindracea*. Leaves and thalli were sampled in a meadow of  
8 *Cymodocea nodosa* invaded by the invasive *Caulerpa cylindracea* and in a monospecific  
9 settlement of *Caulerpa cylindracea* located in the proximity of the meadow at monthly intervals.  
10 For comparison the ambient prokaryotic plankton community was also characterized. Sequencing  
11 results at the OTU level showed a clear differentiation between ambient water and epiphytic  
12 communities and a host-specific community assemblage. In addition, successional changes were  
13 observed that could be connected to the macrophyte growth cycle. Taxonomic analysis showed  
14 similar high rank groups in the ambient water and epiphytic communities, with the exception of  
15 *Desulfobacterota* that were found only on *Caulerpa cylindracea*. Only *Cyanobacteria* showed  
16 seasonal change, while other high rank taxa were present throughout the year. In every analyzed  
17 high rank taxa, phylogenetic groups present throughout the year and comprising most of the  
18 sequences could be identified together with low proportion taxa showing seasonal patterns  
19 connected to the macrophyte growth cycle. Taken together, epiphytic microbial communities  
20 of the seagrass *Cymodocea nodosa* and the macroalgae *Caulerpa cylindracea* appear to be  
21 host-specific and contain taxa that undergo successional changes.

22 **Introduction**

23       Marine macrophytes (seagrasses and macroalgae) are important ecosystem engineers that  
24   form close associations with microorganism belonging to all three domains of life (Egan *et al.*,  
25   2013; Tarquinio *et al.*, 2019). Microbes can live within macrophyte tissue as endophytes or can  
26   form epiphytic communities on surfaces of leaves and thalli (Egan *et al.*, 2013; Hollants *et al.*,  
27   2013; Tarquinio *et al.*, 2019). Epiphytic and endophytic microbial communities form a close  
28   functional relationship with the macrophyte host. It was proposed that this close relationship  
29   constitutes a holobiont, an integrated community where the macrophyte organism and its symbiotic  
30   partners support each other (Margulis, 1991; Egan *et al.*, 2013; Tarquinio *et al.*, 2019).

31       Biofilms formed from microbial epiphytes can contain diverse taxonomic groups and harbor  
32   cell densities from  $10^2$  to  $10^7$  cells  $\text{cm}^{-2}$  (Armstrong *et al.*, 2000; Bengtsson *et al.*, 2010; Burke *et*  
33   *al.*, 2011b). In such an environment a number of positive and negative interactions between the  
34   macrophyte and colonizing microorganisms have been described (Egan *et al.*, 2013; Hollants *et*  
35   *al.*, 2013; Tarquinio *et al.*, 2019). Macrophytes can promote growth of associated microbes by  
36   nutrient exudation, while in return microorganisms may support macrophyte performance through  
37   improved nutrient availability, phytohormone production and protection form toxic compounds,  
38   oxidative stress, biofouling organisms and pathogens (Egan *et al.*, 2013; Hollants *et al.*, 2013;  
39   Tarquinio *et al.*, 2019). Beside this positive interactions, macrophytes can negatively impact  
40   the associated microbes such as pathogenic bacteria by producing reactive oxygen species and  
41   secondary metabolites (Egan *et al.*, 2013; Hollants *et al.*, 2013; Tarquinio *et al.*, 2019).

42       All these ecological roles are carried out by a taxonomically diverse community of  
43   microorganisms. At higher taxonomic ranks a core set of macrophyte epiphytic taxa was  
44   described consisting mainly of *Alphaproteobacteria*, *Gammaproteobacteria*, *Desulfobacterota*,  
45   *Bacteroidota*, *Cyanobacteria*, *Actinobacteriota*, *Firmicutes*, *Planctomycetota*, *Chloroflexi* and  
46   *Verrucomicrobiota* (Crump and Koch, 2008; Tujula *et al.*, 2010; Lachnit *et al.*, 2011). In contrast,

47 at lower taxonomic ranks host specific microbial communities were described (Lachnit *et al.*,  
48 2011; Roth-Schulze *et al.*, 2016). Recently, it was shown that even different morphological niches  
49 within the same alga had a higher influence on bacterial community variation than biogeography  
50 or environmental factors (Morrissey *et al.*, 2019). While there is high community variation  
51 between host species is was observed that the majority of metagenome determined functions were  
52 conserved both between host species and individuals (Burke *et al.*, 2011a; Roth-Schulze *et al.*,  
53 2016). This discrepancy between taxonomic and functional composition could be explained by  
54 the lottery hypothesis. It postulates that an initial random colonization step is performed from  
55 a set of functionally equivalent taxonomic groups resulting in taxonomically different epiphytic  
56 communities sharing a core set of functional genes (Burke *et al.*, 2011a; Roth-Schulze *et al.*,  
57 2016). In addition, some of the variation in the observed data could be attributed to different  
58 techniques used in various studies, such as different protocols for epiphytic cell detachment and/or  
59 DNA isolation, as no standard protocol to study epiphytic communities was established (Ugarelli  
60 *et al.*, 2019; Korlević *et al.*, submitted).

61 The majority of studies describing macrophyte epiphytic communities did not encompass  
62 seasonal changes (Crump and Koch, 2008; Lachnit *et al.*, 2009; Burke *et al.*, 2011b; Roth-Schulze  
63 *et al.*, 2016; Ugarelli *et al.*, 2019). In addition, if seasonal changes were taken into account low  
64 temporal frequency and/or methodologies that do not allow for high taxonomic resolution were  
65 used (Tujula *et al.*, 2010; Lachnit *et al.*, 2011; Miranda *et al.*, 2013; Michelou *et al.*, 2013). In  
66 the present study we describe the seasonal dynamics of bacterial and archaeal communities on  
67 the surfaces of the seagrass *Cymodocea nodosa* and siphonous macroalgae *Caulerpa cylindracea*  
68 determined on a mostly monthly scale. Bacterial and archaeal epiphytes were sampled in a meadow  
69 of *C. nodosa* invaded by the invasive *C. cylindracea* and in a locality of only *C. cylindracea*  
70 located in the proximity of the meadow. In addition, for comparison, the community of the ambient  
71 seawater was characterized.

72 **Results**

73 Sequencing of the 16S rRNA V4 region yielded a total of 1.8 million sequences after  
74 quality curation and exclusion of eukaryotic, chloroplast, mitochondrial and no relative sequences  
75 (Table S1). A total of 35 samples originating from epiphytic archaeal and bacterial communities  
76 associated with surfaces of the seagrass *C. nodosa* and macroalga *C. cylindracea* were analyzed. In  
77 addition, 18 samples (one of the samples was sequenced two times) originating from picoplankton  
78 archaeal and bacterial communities in the ambient seawater were also processed for comparison.  
79 The number of reads per sample ranged between 8,410 and 77,465 sequences (Table S1). Even  
80 when the highest sequencing effort was applied the rarefaction curves did not level off that is a  
81 common observation in high-throughput 16S rRNA amplicon sequencing approaches (Figure S1).  
82 Following quality curation and exclusion of sequences mentioned before reads were clustered  
83 into 28,729 different OTUs at a similarity level of 97 %. Reads numbers were normalized to the  
84 minimum number of sequences, 8,410 (Table S1), through rarefaction resulting in 17,019 different  
85 OTUs that ranged from 355 to 2,018 OTUs per sample (Figure S2). To determine seasonal changes  
86 of richness and diversity the Observed Number of OTUs, Chao1, ACE, Exponential Shannon (Jost,  
87 2006) and Inverse Simpson were calculated after normalization through rarefaction. Generally,  
88 richness estimators and diversity indices showed similar trends. On average, higher values were  
89 found for *C. cylindracea* (invaded [Number of OTUs,  $1,690.5 \pm 152.3$  OTUs] and noninvaded  
90 [Number of OTUs,  $1,733.8 \pm 163.5$  OTUs]), middle values for *C. nodosa* (Number of OTUs,  
91  $1,066.9 \pm 224.5$  OTUs) and lower values for picoplankton communities in the ambient seawater  
92 (Number of OTUs,  $526 \pm 145.6$  OTUs) (Figure S2). Seasonal changes did not show such large  
93 dissimilarities. *C. nodosa* communities showed a slow increase towards the end of the study,  
94 while *C. cylindracea* (invaded and noninvaded) communities were characterized by slightly larger  
95 values in Spring and Summer in comparison to Autumn and Winter (Figure S2).

96 To determine the proportion of shared archaeal and bacterial OTUs and communities sampled  
97 in different environments the Jaccard's Similarity Coefficient on presence-absence data and

98 Bray-Curtis Similarity Coefficient were, respectively, calculated. Coefficients were determined  
99 after normalization through rarefaction and binning of samples from a particular environment. The  
100 highest proportion of shared OTUs and community was found between invaded and noninvaded  
101 *C. cylindracea* (Jaccard, 0.35; Bray-Curtis, 0.77), while lower shared values were calculated  
102 between seawater and epiphytic communities (Figure 1). Shared proportion between *C. nodosa*  
103 and *C. cylindracea* were approximately in the middle between these two extremes. To assess  
104 seasonal changes in the proportion of shared OTUs and communities the Jaccard's and Bray-Curtis  
105 Similarity Coefficients were calculated between consecutive sampling points (Figure 2). Both  
106 coefficients showed similar trends. Temporal proportional changes were more pronounced for  
107 seawater in comparison to *C. nodosa* and especially *C. cylindracea* associated communities  
108 (Figure 2). In addition, only 0.4 – 1.0 % of OTUs from each surface associated community were  
109 found at every time point. These OTUs made also a high proportion of total sequences (39.9  
110 – 52.8 %). To further disentangle the environmental and seasonal community dissimilarity a  
111 Principal Coordinates Analysis (PCoA) based on Bray-Curtis distances and OTU abundances was  
112 applied. It showed a clear separation between planktonic and surface associated communities  
113 (Figure 3). In addition, a separation of epiphytic bacterial and archaeal communities based on  
114 host species was determined. This separation was further supported by ANOSIM ( $R = 0.96, p <$   
115 0.001). Seasonal changes of *C. nodosa* associated communities indicated a separation between  
116 Spring, Summer and Autumn/Winter samples (ANOSIM,  $R = 0.54, p < 0.01$ ), while communities  
117 from the surfaces of *C. cylindracea* indicated a non so strongly supported, as in previous cases,  
118 separation between Summer and Autumn/Winter/Spring samples (ANOSIM,  $R = 0.31, p < 0.05$ )  
119 (Figure 3).

120 The taxonomic composition of both, macrophyte associated and seawater communities,  
121 was dominated by bacterial ( $99.1 \pm 2.1 \%$ ) over archaeal sequences ( $0.9 \pm 2.1 \%$ ) (Figure 4).  
122 Higher relative abundances of chloroplast related sequences were only observed in surface  
123 associated communities, with higher values in Autumn/Winter ( $37.2 \pm 11.2 \%$ ) in comparison to  
124 Spring/Summer ( $20.9 \pm 9.7 \%$ ) (Figure S3). Generally, at higher taxonomic ranks (phylum-class)

125 epiphytic and seawater microbial communities were composed of similar bacterial taxa.  
126 Seawater communities were mainly comprised of *Actinobacteriota*, *Bacteroidota*, *Cyanobacteria*,  
127 *Alphaproteobacteria*, *Gammaproteobacteria* and *Verrucomicrobiota*. Communities associated  
128 with *C. nodosa* were consisted of same groups with the addition of *Planctomycetota* whose  
129 contribution was higher in summer 2018. In addition, communities from invaded and noninvaded  
130 *C. cylindracea* were similar and characterized by same groups as seawater and *C. nodosa*  
131 communities with the addition of *Desulfobacterota* (Figure 4). Larger differences between  
132 environments and host species could be observed at lower taxonomic ranks (Figure 5 – 9).

133 *Cyanobacteria* related sequences were comprising, on average,  $5.5 \pm 4.4$  % of total sequences  
134 (Figure 5). Higher proportions were found for *C. nodosa* ( $16.4 \pm 5.3$  %) and *C. cylindracea*  
135 (invaded [ $(7.7 \pm 3.9$  %]) and noninvaded [ $(7.8 \pm 2.4$  %)]) associated communities in autumn and  
136 for seawater communities in winter ( $8.8 \pm 7.4$  %). Large taxonomic differences between surface  
137 associated and seawater cyanobacterial communities were observed. Seawater communities  
138 were mainly comprised of *Cyanobium* and *Synechococcus*, while surface associated communities  
139 were consisted of *Pleurocapsa* and sequences without known relatives within *Cyanobacteriia*  
140 (Figure 5). In addition, seasonal changes in surface associated communities were observed  
141 with *Pleurocapsa* and no relative *Cyanobacteriia* comprising larger proportions in autumn and  
142 winter and *Acrophormium*, *Phormidesmis* and no relative *Nodosilineaceae* in spring and summer  
143 (Figure 5).

144 Sequences classified as *Bacteroidota* were comprising, on average,  $19.2 \pm 5.5$  % of all  
145 sequences (Figure 6). Similarly to *Cyanobacteria*, large differences in the taxonomic composition  
146 between seawater and surface associated communities were found (Figure 6). The seawater  
147 community was characterized by the NS4 and NS5 marine groups, uncultured *Cryomorphaceae*,  
148 uncultured *Flavobacteriaceae*, NS11-12 marine group, *Balneola*, uncultured *Balneolaceae* and  
149 *Formosa*. In contrast, in surface associated communities *Lewinella*, *Portibacter*, *Rubidimonas*, no  
150 relative *Sapspiraceae*, uncultured *Sapspiraceae*, no relative *Flavobacteriaceae* and uncultured

151 *Rhodothermaceae* were found. Some groups showed slight seasonal changes such as no relative  
152 *Flavobacteriaceae* that were more pronounced from November 2017 until June 2018. In contrast,  
153 uncultured *Rhodothermaceae* showed higher proportions from June 2018 until the end of the study  
154 period. Surface associated *Bacteroidota* communities were very diverse as could be observed in  
155 the the high proportion of taxa that grouped as other *Bacteroidota* (Figure 6).

156 On average, *Alphaproteobacteria* were in comparison to other high rank taxa the largest  
157 taxonomic group, comprising  $29.2 \pm 12.0$  % of all sequences (Figure 7). In accordance to previous  
158 taxa, high differences between seawater and surface associated communities were observed.  
159 Picoplankton communities were composed mainly of the SAR11 clade, AEGEAN-169 marine  
160 group, SAR116 clade, no relative *Rhodobacteraceae*, HIMB11 and OCS116 clade, while surface  
161 associated communities were composed in high proportion of no relative *Rhodobacteraceae* and to  
162 a lesser degree of *Pseudoahrensia*, no relative *Alphaproteobacteria*, no relative *Hyphomonadaceae*  
163 and *Amylibacter*. Representatives of no relative *Rhodobacteraceae* were comprising on average  
164  $40.6 \pm 23.2$  % of all alphaproteobacterial sequences from the epiphytic community (Figure 7). In  
165 addition, *Amylibacter* was detected mainly in *C. nodosa* from November 2017 until March 2018.

166 Sequences related to *Gammaproteobacteria* were comprising, on average,  $18.7 \pm 3.9$  %  
167 of all sequences (Figure 8). Similarly to previous taxa, large taxonomic differences between  
168 seawater and surface associated communities were found. Seawater communities were mainly  
169 comprised of the OM60 (NOR5) clade, *Litoricola*, *Acinetobacter* and the SAR86 clade,  
170 while epiphytic communities were mainly composed of no relative *Gammaproteobacteria* and  
171 *Granulosicoccus*. Beside these two groups specific to all three epiphytic communities, *C. nodosa*  
172 was characterized by *Arenicella*, no relative *Burkholderiales* and *Methylotenera*, while *Thioploca*,  
173 no relative *Cellvibrionaceae* and *Reinekea* were more specific to both invaded and noninvaded  
174 *C. cylindracea*. In addition, *Arenicella* was more pronounced in November and December 2017,  
175 while no relative *Burkholderiales* and *Methylotenera* were more characteristic for the period form  
176 March until May 2018. For the *C. cylindracea* specific taxa no relative *Cellvibrionaceae* and

<sup>177</sup> *Reinekea* showed some seasonality and were characterisitic for samples originating from June to  
<sup>178</sup> October 2018. In addition, similarly to *Bacteroidota*, a large proportion of the surface associated  
<sup>179</sup> community was grouped as other *Gammaproteobacteria* indicating high diversity within this  
<sup>180</sup> group (Figure 8).

<sup>181</sup> In contrast to previously described high rank taxa, *Desulfobacterota* were specific to  
<sup>182</sup> *C. cylindracea*. On average they were comprising  $11.2 \pm 13.3$  % of all sequences. While  
<sup>183</sup> seawater and *C. nodosa* communities were consisted of only  $0.1 \pm 0.08$  % and  $1.0 \pm 0.7$   
<sup>184</sup> % *Desulfobacterota* sequences, respectively, in the invaded and noninvaded *C. cylindracea*  
<sup>185</sup> communities their proportion was  $25.7 \pm 11.2$  % and  $24.0 \pm 4.3$  %, respectively (Figure 9). The  
<sup>186</sup> community was mainly consisted of no relative *Desulfobacteraceae*, *Desulfatitalea*, no relative  
<sup>187</sup> *Desulfobulbaceae*, *Desulfobulbus*, no relative *Desulfocapsaceae*, *Desulfopila*, *Desulforhopalus*,  
<sup>188</sup> *Desulfotalea*, SEEP-SRB4 and uncultured *Desulfocapsaceae* (Figure 9).

189 **Discussion**

190 Surfaces of marine macrophytes are harboring biofilms consisted of diverse microbial taxa  
191 (Egan *et al.*, 2013; Tarquinio *et al.*, 2019). No standard protocol has been developed to study  
192 these macophyte associated microbes (Ugarelli *et al.*, 2019). Different procedures of microbial  
193 cells removal from host surfaces were described, such as host tissue shaking (Nõges *et al.*, 2010),  
194 scraping (Uku *et al.*, 2007) and ultrasonication (Cai *et al.*, 2014). All these methods showed  
195 different removal efficiencies but none was enabling a complete removal of attached microbial  
196 cells. In the present study, we applied an earlier developed removal protocol (Korlević *et al.*,  
197 submitted), based on a previous idea of direct cellular lysis (Burke *et al.*, 2009), to ensure an  
198 almost complete cell detachment. The application of a direct lysis procedure coupled with a high  
199 frequency sampling protocol and Illumina high resolution amplicon sequencing has enabled us to  
200 make a detailed description of bacterial and archaeal communities associated with the surfaces of  
201 two marine macrophytes, *C. nodosa* and *C. cylindracea*.

202 In the present study, highest richness values were observed for *C. cylindracea* (invaded and  
203 noninvaded), middle for *C. nodosa* and lowest for seawater derived communities. Higher values  
204 for seagrass associated communities in comparison to seawater were described earlier and could  
205 be attributed to a larger set of inhabitable microniches existing on macrophyte surfaces (Ugarelli  
206 *et al.*, 2019). In addition, highest values observed for *C. cylindracea* are probably a consequence  
207 of part of epiphytic OTUs that are in contact with the sediment. *C. cylindracea* stolon is attached  
208 to the sediment surface with rhizoids, so the stolon and rhizoids are in a direct contact with the  
209 sediment. Part of the surface attached *Caulerpa cylindracea* community is therefore comprised of  
210 OTUs that are in contact with a different environment and that could cause the observed increase  
211 in richness. In addition, seasonal richness differences observed for surface attached communities  
212 showed slightly higher values in spring and summer. This pattern could be explained by a higher  
213 macrophyte growth in these seasons (M. Najdek, personal communication; Zavodnik *et al.*,  
214 1998; Ruitton *et al.*, 2005). During active periods macrophytes exhibit a more dynamic chemical

215 interaction with the surface community probably causing an increase in the number of inhabitable  
216 microniches (Borges and Champenois, 2015; Rickert *et al.*, 2016).

217 Since the colonization of macrophyte surfaces is performed from a pool of seawater  
218 prokaryotic cells it is interesting to see to which extent do these two communities differ. We  
219 observed a strong differentiation between the surface attached and seawater communities at the  
220 level of OTUs that is in agreement with most published studies (Burke *et al.*, 2011b; Michelou  
221 *et al.*, 2013; Roth-Schulze *et al.*, 2016; Crump *et al.*, 2018; Ugarelli *et al.*, 2019). These data  
222 indicate that marine macrophytes are selecting, from a pool of seawater microbial taxa, the one  
223 that can colonize and proliferate on their surfaces (Salaün *et al.*, 2012; Michelou *et al.*, 2013). In  
224 contrast to these findings Fahimipour *et al.* (2017) found, in a global study of *Zostera marina*,  
225 similarities between leaves and seawater samples. Discrepancies between our data and this  
226 study could be explained by differences in studied seagrass species, methodological variations or  
227 biogeographic trends as Fahimipour *et al.* (2017) were analyzing samples from different locations  
228 throughout the northern hemisphere. It is possible that ambient seawater and leaves communities  
229 from the same location are differing but are still more similar to each other when compared to  
230 other sampling locations. Indeed, it was found that prokaryotic communities vary substantially  
231 between different sampling sites (Bengtsson *et al.*, 2017). When the taxonomic composition at  
232 high ranks was analyzed no such strong differentiation was noticed. Phyla and classes such as:  
233 *Actinobacteriota*, *Bacteroidota*, *Cyanobacteria*, *Alphaproteobacteria*, *Gammaproteobacteria* and  
234 *Verrucomicrobiota*, were described that is in agreement with previously reported data (Burke *et*  
235 *al.*, 2011b; Egan *et al.*, 2013; Michelou *et al.*, 2013). In contrast, when low taxonomic ranks were  
236 analyzed (i.g. family and genus) a strong differentiation was observed. A similar differentiation  
237 at lower taxonomic ranks was described for other species of macrophytes (Egan *et al.*, 2013;  
238 Michelou *et al.*, 2013; Ugarelli *et al.*, 2019).

239 Beside differences between seawater and surface associated communities, there were  
240 discussions if the prokaryotic epiphytic community is host-specific or there are generalists taxa

characteristic to all or many macrophytes (Egan *et al.*, 2013). Similarly to previously described differences between seawater and surface attached communities, at high taxonomic ranks no strong differentiation between communities associated with different host was observed. The only high rank phylum that was differing between *C. nodosa* and *C. cylindracea* was *Desulfobacterota*, whose sequences were more abundant in the *C. cylindracea* associated community. As already mentioned, the rhizoids and part of the stolon are in contact with the sediment, so *Desulfobacterota* are probably a part of the epiphytic community that is in contact with the sediment. Similar high rank taxa found in this study were described to be specific for other species of macrophytes (Burke *et al.*, 2011b; Lachnit *et al.*, 2011; Bengtsson *et al.*, 2017). In contrast to high taxonomic ranks, a substantial differentiation between host specific communities was found, which supports the host-specific hypothesis. Similar host-specificity was observed for different species of macroalgae and seagrasses (Lachnit *et al.*, 2011; Roth-Schulze *et al.*, 2016; Ugarelli *et al.*, 2019; Morrissey *et al.*, 2019). Taken together, at high taxonomic ranks a core set of taxa could be described that is characteristic for all or many macrophytes, while at low taxonomic ranks a community specific to host species could be identified (Egan *et al.*, 2013).

Seasonal richness changes in the epiphytic community were substantial as could be observed in the proportion of OTUs that could be found at every sampling time ( $\leq 1.0\%$ ). Interestingly, these OTUs were accounting for a high proportion of sequences ( $\leq 52.8\%$ ). A very similar proportion of persistent OTUs and their sequence contribution was reported in high frequency studies describing seasonal picoplankton changes (Gilbert *et al.*, 2009, 2012). In comparison to the seawater community, a lower degree of seasonal shifts was observed for the surface associated communities. It seems, that microniches on the surfaces of macrophytes are providing more stable conditions in comparison to the seawater. At the level of OTUs seasonal changes of *C. nodosa* and *C. cylindracea* associated communities were identified that could be linked to the growth cycle of the seagrass and macroalgae (M. Najdek, personal communication). *C. nodosa* was characterized by a Spring community during maximum seagrass proliferation, a Summer community during a biomass maximum and a Autumn/Winter community during a biomass

268 decay. In contrast, *C. cylindracea* started to proliferate in late Spring and was characterized only  
269 by a Summer community during maximal biomass increase and by a Autumn/Winter/Spring  
270 community when the biomass were at the peak and the settlement started to subsequently decay.  
271 Similar seasonal changes in the epiphytic community was described also for other macroalgae  
272 (Tujula *et al.*, 2010; Lachnit *et al.*, 2011). Higher temporal stability of *C. cylindracea* surface  
273 communities in comparison to *C. nodosa* were also observed in the higher proportion of shared  
274 communities between two consecutive sampling points.

275 Analysis of seasonal chloroplast sequence abundances showed higher values in Autumn/Winter  
276 in comparison to Spring/Summer. This pattern is not surprising as e.g seagrasses are known to  
277 harbor more epiphytes during Autumn/Winter (Reyes and Sansón, 2001) and we used an adapted  
278 DNA isolation protocol that is known to partially coextract DNA from planktonic eukaryotes  
279 (Korlević *et al.*, 2015). Strong seasonal fluctuations of high rank epiphytic taxa were not  
280 observed, with the exception of *Cyanobacteria*. Cyanobacterial sequences were more pronounced  
281 in November and December in comparison to Spring and Summer. Interestingly, in these high  
282 proportion months the majority of cyanobacterial sequences were classified as *Pleurocapsa*, a  
283 group known to colonized different living and nonliving surfaces (Burns *et al.*, 2004; Longford *et*  
284 *al.*, 2007; Mobberley *et al.*, 2012; Reisser *et al.*, 2014). It is possible than during periods of low  
285 metabolic activity there is no so active interaction and selection of the epiphytic community by  
286 the seagrass, causing leaves to become a suitable surface for nonspecific colonizers (Zavodnik *et*  
287 *al.*, 1998). *Pleurocapsa* was replaced in Spring and Summer by *Acrophormium*, *Phormidesmis*  
288 and no relative *Nodosilineaceae*. A study of coastal microbial mats found also higher proportion  
289 of *Nodosilineaceae* sequences in Summer, while *Phormidesmis* sequences were at their peak in  
290 Autumn (Cardoso *et al.*, 2019). Other high rank taxa did not showed strong successional patterns,  
291 but in every analyzed group, with the exception of *Desulfobacterota*, taxa present throughout  
292 the year in similar proportions and season specific taxa could be identified. Within *Bacteroidota*  
293 different groups withing the family *Saprospiraceae* (i.g. *Lewinella*, *Portibacter* and *Rubidimonas*)  
294 were detected through the year. Members of this family are often found in association with

macrophytes and it is suggested that are involved in the hydrolysis and utilization of complex carbon sources (Burke *et al.*, 2011b; McIlroy and Nielsen, 2014; Crump *et al.*, 2018). On the other hand, families *Flavobacteriaceae* and *Rhodothermaceae* showed seasonal patterns, with *Flavobacteriaceae* being more pronounced from November to June and *Rhodothermaceae* from June to October. Within *Alphaproteobacteria* the family *Rhodobacteraceae* was comprising the majority of sequences thought the year. This metabolically versatile family is often associated with macrophyte surfaces and usually is one of the most abundant groups (Burke *et al.*, 2011b; Michelou *et al.*, 2013; Pujalte *et al.*, 2014). In addition, *Hyphomonadaceae* were found in all samples. Interestingly, some of the species within this group contain stalks on their cells which can be used to attach to the macrophyte surface (Weidner *et al.*, 2000; Abraham and Rohde, 2014). Within the *Gammaproteobacteria*, sequences without known representatives were the most pronounced group present throughout the year. In addition, *Granulosicoccus* was also found in almost all samples. *Gammaproteobacteria* are often a major constituent of macrophyte epiphytic communities (Burke *et al.*, 2011b; Michelou *et al.*, 2013; Crump *et al.*, 2018). Beside these two groups other less pronounced taxa showed seasonal and host-specific patterns. In example, *C. cylindracea* was characterized by *Thioploca*, a known sulfur sediment bacteria and *Cellvibrionaceae*, a family whose cultured members are known polysaccharides degraders (Jørgensen and Gallardo, 1999; Xie *et al.*, 2017). *Desulfobacterota* were found only associated with *C. cylindracea* and no group within this phylum showed seasonal patterns. The presence of this phylum only on *C. cylindracea* is to be expected as part of the epiphytic community is in a direct contact with the sediment. The *Desulfobacterota* community was dominated by *Desulfatitalea* and no relative *Desulfocapsaceae*, known sulfate sediment groups (Kuever, 2014; Higashioka *et al.*, 2015).

In temperate zones marine macrophytes are exhibiting growth cycles, so it is not surprising that the associated epiphytic microbial community is undergoing partial seasonal changes. In the present study, we could, in every analyzed high rank taxa, identify phylogenetic groups that were present throughout the year and that were comprising most of the sequences and lower

322 proportion taxa showing seasonal patterns connected to the macrophyte growth cycle. Studies  
323 focusing on functional comparisons between communities associated with different hosts showed  
324 that the majority of functions could be found in every community, indicating functional redundancy  
325 (Roth-Schulze *et al.*, 2016). This difference between taxonomic and functional discrepancy was  
326 explained by the lottery hypothesis that hypothesize an initial random colonization step performed  
327 from a set of functionally equivalent taxonomic groups (Burke *et al.*, 2011a; Roth-Schulze *et al.*,  
328 2016). It is possible that functional redundancy is a characteristic of high abundance taxa detected  
329 to be present throughout the year, while seasonal and/or host-specific functions are an attribute  
330 of taxa displaying successional patterns. Further studies connecting taxonomy with functional  
331 properties will be required to elucidate the degree of functional redundancy or specificity in  
332 epiphytic microbial communities.

333 **Experimental Procedures**

334 **Sampling**

335 Leaves of *C. nodosa* were sampled in a *C. nodosa* meadow located in the proximity of the  
336 village of Funtana (45°10'39" N, 13°35'42" E). Thalli of *C. cylindracea* were sampled in the  
337 same *C. nodosa* invaded meadow in Funtana and on a locality of only *C. cylindracea* located  
338 close to the invaded meadow. Sampling of leaves and thalli was performed approximately monthly  
339 from December 2017 to October 2018 (Table S1). Leaves and thalli were collected by diving  
340 and transported to the laboratory in containers placed on ice and filled with site seawater. Upon  
341 arrival to the laboratory, *C. nodosa* leaves were cut into sections of 1 – 2 cm, while *C. cylindracea*  
342 thalli were cut into 5 – 8 cm long sections. Leaves and thalli were washed three times with  
343 sterile artificial seawater (ASW) to remove loosely attached microbial cells. Ambient seawater was  
344 collected in 10 l containers by diving and transported to the laboratory where the whole container  
345 volume was filtered through a 20 µm net. The filtrate was further sequentially filtered through 3  
346 µm and 0.2 µm polycarbonate membrane filters (Whatman, United Kingdom) using a peristaltic  
347 pump. Filters were briefly dried at room temperature and stored at –80 °C. Seawater samples were  
348 also collected approximately monthly from July 2017 to October 2018.

349 **DNA Isolation**

350 DNA from surfaces of *C. nodosa* and *C. cylindracea* was isolated using a previously modified  
351 and adapted protocol that allows for a selective epiphytic DNA isolation (Massana *et al.*, 1997;  
352 Korlević *et al.*, submitted). Briefly, leaves and thalli are incubated in a lysis buffer and treated with  
353 lysozyme and proteinase K. Following the incubations, the mixture containing lysed epiphytic cells  
354 is separated from leaves and thalli and extracted using a phenol-chloroform procedure. Finally, the  
355 extracted DNA is precipitated using isopropanol. DNA from seawater picoplankton was isolated

356 from 0.2 µm polycarbonate filters according to (Massana *et al.*, 1997) with a slight modification.  
357 Following the phenol-chloroform extraction steps 1/10 of chilled 3 M sodium acetate (pH 5.2) was  
358 added. DNA was precipitated by adding 1 volume of chilled isopropanol, incubating the mixtures  
359 overnight at -20 °C and centrifuging at 20,000 × g and 4 °C for 21 min. The pellet was washed  
360 twice with 500 µl of chilled 70 % ethanol and centrifuged after each washing step at 20,000 × g  
361 and 4 °C for 5 min. Dried pellets were resuspended in 50 – 100 µl of deionized water.

362 **Illumina 16S rRNA Sequencing**

363 Illumina MiSeq sequencing of the V4 16S rRNA region was performed as described  
364 previously (Korlević *et al.*, submitted). The V4 region of the 16S rRNA gene was amplified using  
365 a two-step PCR procedure. In the first PCR the 515F (5'-GTGYCAGCMGCCGCGTAA-3')  
366 and 806R (5'-GGACTACNVGGGTWTCTAAT-3') primers from the Earth Microbiome Project  
367 (<http://press.igsb.anl.gov/earthmicrobiome/protocols-and-standards/16s/>) were used (Caporaso  
368 *et al.*, 2012; Apprill *et al.*, 2015; Parada *et al.*, 2016). These primers contained on their 5' end  
369 a tagged sequence. Purified PCR products were sent for Illumina MiSeq sequencing at IMGM  
370 Laboratories, Martinsried, Germany. Before sequencing at IMGM, the second PCR amplification  
371 of the two-step PCR procedure was performed using primers targeting the tagged region  
372 incorporated in the first PCR. In addition, these primers contained adapter and sample-specific  
373 index sequences. Beside samples, a positive and negative control for each sequencing batch was  
374 sequenced. Negative control was comprised of PCR reactions without DNA template, while for a  
375 positive control a mock community composed of evenly mixed DNA material originating from 20  
376 bacterial strains (ATCC MSA-1002, ATCC, USA) was used. The sequences obtained in this study  
377 have been submitted to the European Nucleotide Archive (ENA) under accession numbers **TO BE**  
378 **ADDED LATER!**

379 **Sequence Analysis**

380       Obtained sequences were analyzed on the computer cluster Isabella (University Computing  
381       Center, University of Zagreb) using mothur (version 1.43.0) (Schloss *et al.*, 2009) according  
382       to the MiSeq Standard Operating Procedure (MiSeq SOP; [https://mothur.org/wiki/MiSeq\\_SOP](https://mothur.org/wiki/MiSeq_SOP))  
383       (Kozich *et al.*, 2013) and recommendations given from the Riffomonas project to enhance data  
384       reproducibility (<http://www.riffomonas.org/>). For alignment and classification of sequences the  
385       SILVA SSU Ref NR 99 database (release 138; <http://www.arb-silva.de>) was used (Quast *et*  
386       *al.*, 2013; Yilmaz *et al.*, 2014). Pipeline data processing and visualization was done using R  
387       (version 3.6.0) (R Core Team, 2019), packages vegan (version 2.5-6) (Oksanen *et al.*, 2019), and  
388       tidyverse (version 1.3.0) (Wickham *et al.*, 2019) and multiple other packages (Xie, 2014, 2015,  
389       2019a, 2019b, 2020; Neuwirth, 2014; Xie *et al.*, 2018; Allaire *et al.*, 2019; Zhu, 2019). The  
390       detailed analysis procedure including the R Markdown file for this paper are available as a GitHub  
391       repository ([https://github.com/mkorlevic/Korlevic\\_EpiphyticDynamics\\_EnvironMicrobiol\\_2020](https://github.com/mkorlevic/Korlevic_EpiphyticDynamics_EnvironMicrobiol_2020)).  
392       Based on the ATCC MSA-1002 mock community included in the analysis an average sequencing  
393       error rate of 0.01 % was determined, which is in line with previously reported values for  
394       next-generation sequencing data (Kozich *et al.*, 2013; Schloss *et al.*, 2016). In addition, the  
395       negative controls processed together with the samples yielded on average only 2 sequences after  
396       sequence quality curation.

397 **Acknowledgments**

398       This work was founded by the Croatian Science Foundation through the MICRO-SEAGRASS  
399       project (IP-2016-06-7118). We would like to thank Margareta Buterer for technical support, Paolo  
400       Paliaga for help during sampling and the University Computing Center of the University of Zagreb  
401       for access to the cluster Isabella.

402 **References**

- 403 Abraham, W.R. and Rohde, M. (2014) The Family Hyphomonadaceae. In, *The prokaryotes: Alphaproteobacteria and betaproteobacteria*. Springer-Verlag Berlin Heidelberg, pp. 283–299.
- 404
- 405 Allaire, J.J., Xie, Y., McPherson, J., Luraschi, J., Ushey, K., Atkins, A., et al. (2019) rmarkdown: Dynamic Documents for R.
- 406
- 407 Apprill, A., McNally, S., Parsons, R., and Weber, L. (2015) Minor revision to V4 region
- 408 SSU rRNA 806R gene primer greatly increases detection of SAR11 bacterioplankton. *Aquatic*
- 409 *Microbial Ecology* **75**: 129–137.
- 410 Armstrong, E., Rogerson, A., and Leftley, J.W. (2000) The Abundance of Heterotrophic
- 411 Protists Associated with Intertidal Seaweeds. *Estuarine, Coastal and Shelf Science* **50**: 415–424.
- 412 Bengtsson, M.M., Bühler, A., Brauer, A., Dahlke, S., Schubert, H., and Blindow, I. (2017)
- 413 Eelgrass Leaf Surface Microbiomes Are Locally Variable and Highly Correlated with Epibiotic
- 414 Eukaryotes. *Frontiers in Microbiology* **8**: 1312.
- 415 Bengtsson, M., Sjøtun, K., and Øvreås, L. (2010) Seasonal dynamics of bacterial biofilms on
- 416 the kelp *Laminaria hyperborea*. *Aquatic Microbial Ecology* **60**: 71–83.
- 417 Borges, A.V. and Champenois, W. (2015) Seasonal and spatial variability of dimethylsulfoniopropionate
- 418 (DMSP) in the Mediterranean seagrass *Posidonia oceanica*. *Aquatic Botany* **125**: 72–79.
- 419 Burke, C., Kjelleberg, S., and Thomas, T. (2009) Selective extraction of bacterial DNA from
- 420 the surfaces of macroalgae. *Applied and environmental microbiology* **75**: 252–256.
- 421 Burke, C., Steinberg, P., Rusch, D., Kjelleberg, S., and Thomas, T. (2011a) Bacterial
- 422 community assembly based on functional genes rather than species. *Proceedings of the National*
- 423 *Academy of Sciences of the United States of America* **108**: 14288–14293.

- 424 Burke, C., Thomas, T., Lewis, M., Steinberg, P., and Kjelleberg, S. (2011b) Composition,  
425 uniqueness and variability of the epiphytic bacterial community of the green alga *Ulva australis*.  
426 *The ISME journal* **5**: 590–600.
- 427 Burns, B.P., Goh, F., Allen, M., and Neilan, B.A. (2004) Microbial diversity of extant  
428 stromatolites in the hypersaline marine environment of Shark Bay, Australia. *Environmental*  
429 *Microbiology* **6**: 1096–1101.
- 430 Cai, X., Gao, G., Yang, J., Tang, X., Dai, J., Chen, D., and Song, Y. (2014) An ultrasonic  
431 method for separation of epiphytic microbes from freshwater submerged macrophytes. *Journal of*  
432 *basic microbiology* **54**: 758–761.
- 433 Caporaso, J.G., Lauber, C.L., Walters, W.A., Berg-Lyons, D., Huntley, J., Fierer, N., et al.  
434 (2012) Ultra-high-throughput microbial community analysis on the Illumina HiSeq and MiSeq  
435 platforms. *The ISME Journal* **6**: 1621–1624.
- 436 Cardoso, D.C., Cretoiu, M.S., Stal, L.J., and Bolhuis, H. (2019) Seasonal development of a  
437 coastal microbial mat. *Scientific Reports* **9**: 1–14.
- 438 Crump, B.C. and Koch, E.W. (2008) Attached bacterial populations shared by four species of  
439 aquatic angiosperms. *Applied and environmental microbiology* **74**: 5948–5957.
- 440 Crump, B.C., Wojahn, J.M., Tomas, F., and Mueller, R.S. (2018) Metatranscriptomics and  
441 amplicon sequencing reveal mutualisms in seagrass microbiomes. *Frontiers in Microbiology* **9**:
- 442 Egan, S., Harder, T., Burke, C., Steinberg, P., Kjelleberg, S., and Thomas, T. (2013) The  
443 seaweed holobiont: understanding seaweed-bacteria interactions. *FEMS microbiology reviews* **37**:  
444 462–476.
- 445 Fahimipour, A.K., Kardish, M.R., Lang, J.M., Green, J.L., Eisen, J.A., and Stachowicz, J.J.  
446 (2017) Globalscale structure of the eelgrass microbiome. *Applied and Environmental Microbiology*

447 83:

448 Gilbert, J.A., Field, D., Swift, P., Newbold, L., Oliver, A., Smyth, T., et al. (2009) The  
449 seasonal structure of microbial communities in the Western English Channel. *Environmental*  
450 *Microbiology* **11**: 3132–3139.

451 Gilbert, J.A., Steele, J.A., Caporaso, J.G., Steinbrück, L., Reeder, J., Temperton, B., et al.  
452 (2012) Defining seasonal marine microbial community dynamics. *The ISME Journal* **6**: 298–308.

453 Higashioka, Y., Kojima, H., Watanabe, T., and Fukui, M. (2015) Draft genome sequence of  
454 *Desulfatitalea tepidiphila* S28bFT. *Genome Announcements* **3**:

455 Hollants, J., Leliaert, F., De Clerck, O., and Willems, A. (2013) What we can learn from  
456 sushi: A review on seaweed-bacterial associations. **83**: 1–16.

457 Jost, L. (2006) Entropy and diversity. **113**: 363–375.

458 Jørgensen, B.B. and Gallardo, V.A. (1999) *Thioploca* spp.: filamentous sulfur bacteria with  
459 nitrate vacuoles. *FEMS Microbiology Ecology* **28**: 301–313.

460 Korlević, M., Markovski, M., Zhao, Z., Herndl, G.J., and Najdek, M. Selective DNA and  
461 Protein Isolation from Marine Macrophyte Surfaces.

462 Korlević, M., Pop Ristova, P., Garić, R., Amann, R., and Orlić, S. (2015) Bacterial Diversity in  
463 the South Adriatic Sea during a Strong, Deep Winter Convection Year. *Applied and Environmental*  
464 *Microbiology* **81**: 1715–1726.

465 Kozich, J.J., Westcott, S.L., Baxter, N.T., Highlander, S.K., and Schloss, P.D. (2013)  
466 Development of a dual-index sequencing strategy and curation pipeline for analyzing amplicon  
467 sequence data on the MiSeq Illumina sequencing platform. *Applied and environmental*  
468 *microbiology* **79**: 5112–5120.

- 469        Kuever, J. (2014) The Family Desulfobulbaceae. In, *The prokaryotes: Deltaproteobacteria*  
470    and *epsilonproteobacteria*. Springer-Verlag Berlin Heidelberg, pp. 75–86.
- 471        Lachnit, T., Blümel, M., Imhoff, J.F., and Wahl, M. (2009) Specific epibacterial communities  
472    on macroalgae: Phylogeny matters more than habitat. *Aquatic Biology* **5**: 181–186.
- 473        Lachnit, T., Meske, D., Wahl, M., Harder, T., and Schmitz, R. (2011) Epibacterial community  
474    patterns on marine macroalgae are host-specific but temporally variable. *Environmental*  
475    *Microbiology* **13**: 655–665.
- 476        Longford, S., Tujula, N., Crocetti, G., Holmes, A., Holmström, C., Kjelleberg, S., et al. (2007)  
477    Comparisons of diversity of bacterial communities associated with three sessile marine eukaryotes.  
478    *Aquatic Microbial Ecology* **48**: 217–229.
- 479        Margulis, L. (1991) Symbiogenesis and symbioticism. In, Margulis,L. and Fester,R. (eds),  
480    *Symbiosis as a source of evolutionary innovation*. Cambridge, Massachusetts: The MIT Press, pp.  
481    1–14.
- 482        Massana, R., Murray, A.E., Preston, C.M., and DeLong, E.F. (1997) Vertical distribution and  
483    phylogenetic characterization of marine planktonic Archaea in the Santa Barbara Channel. *Applied*  
484    *and environmental microbiology* **63**: 50–56.
- 485        McIlroy, S.J. and Nielsen, P.H. (2014) The Family Saprospiraceae. In, *The prokaryotes: Other*  
486    *major lineages of bacteria and the archaea*. Springer-Verlag Berlin Heidelberg, pp. 863–889.
- 487        Michelou, V.K., Caporaso, J.G., Knight, R., and Palumbi, S.R. (2013) The Ecology of  
488    Microbial Communities Associated with *Macrocystis pyrifera*. *PLoS ONE* **8**: e67480.
- 489        Miranda, L.N., Hutchison, K., Grossman, A.R., and Brawley, S.H. (2013) Diversity and  
490    Abundance of the Bacterial Community of the Red Macroalga *Porphyra umbilicalis*: Did Bacterial  
491    Farmers Produce Macroalgae? *PLoS ONE* **8**: e58269.

- 492        Mobberley, J.M., Ortega, M.C., and Foster, J.S. (2012) Comparative microbial diversity  
493        analyses of modern marine thrombolitic mats by barcoded pyrosequencing. *Environmental*  
494        *Microbiology* **14**: 82–100.
- 495        Morrissey, K.L., Çavas, L., Willems, A., and De Clerck, O. (2019) Disentangling the influence  
496        of environment, host specificity and thallus differentiation on bacterial communities in siphonous  
497        green seaweeds. *Frontiers in Microbiology* **10**:
- 498        Neuwirth, E. (2014) RColorBrewer: ColorBrewer Palettes.
- 499        Nõges, T., Luup, H., and Feldmann, T. (2010) Primary production of aquatic macrophytes  
500        and their epiphytes in two shallow lakes (Peipsi and Võrtsjärv) in Estonia. *Aquatic Ecology* **44**:  
501        83–92.
- 502        Oksanen, J., Blanchet, F.G., Friendly, M., Kindt, R., Legendre, P., McGlinn, D., et al. (2019)  
503        vegan: Community Ecology Package.
- 504        Parada, A.E., Needham, D.M., and Fuhrman, J.A. (2016) Every base matters: assessing small  
505        subunit rRNA primers for marine microbiomes with mock communities, time series and global  
506        field samples. *Environmental Microbiology* **18**: 1403–1414.
- 507        Pujalte, M.J., Lucena, T., Ruvira, M.A., Arahal, D.R., and Macián, M.C. (2014) The  
508        family Rhodobacteraceae. In, *The prokaryotes: Alphaproteobacteria and betaproteobacteria*.  
509        Springer-Verlag Berlin Heidelberg, pp. 439–512.
- 510        Quast, C., Pruesse, E., Yilmaz, P., Gerken, J., Schweer, T., Yarza, P., et al. (2013) The SILVA  
511        ribosomal RNA gene database project: improved data processing and web-based tools. *Nucleic*  
512        *acids research* **41**: D590–6.
- 513        R Core Team (2019) R: A Language and Environment for Statistical Computing, Vienna,  
514        Austria: R Foundation for Statistical Computing.

- 515 Reisser, J., Shaw, J., Hallegraeff, G., Proietti, M., Barnes, D.K.A., Thums, M., et al. (2014)
- 516 Millimeter-sized marine plastics: a new pelagic habitat for microorganisms and invertebrates. *PLoS*
- 517 **one** **9**: e100289.
- 518 Reyes, J. and Sansón, M. (2001) Biomass and production of the epiphytes on the leaves of
- 519 *Cymodocea nodosa* in the Canary Islands. *Botanica Marina* **44**: 307–313.
- 520 Rickert, E., Wahl, M., Link, H., Richter, H., and Pohnert, G. (2016) Seasonal variations in
- 521 surface metabolite composition of *fucus vesiculosus* and *fucus serratus* from the Baltic Sea. *PLoS*
- 522 **ONE** **11**:
- 523 Roth-Schulze, A.J., Zozaya-Valdés, E., Steinberg, P.D., and Thomas, T. (2016) Partitioning of
- 524 functional and taxonomic diversity in surface-associated microbial communities. *Environmental*
- 525 *microbiology* **18**: 4391–4402.
- 526 Ruitton, S., Verlaque, M., and Boudouresque, C.F. (2005) Seasonal changes of the introduced
- 527 *Caulerpa racemosa* var. *cylindracea* (Caulerpales, Chlorophyta) at the northwest limit of its
- 528 Mediterranean range. *Aquatic Botany* **82**: 55–70.
- 529 Salaün, S., Barre, S. la, Santos-Goncalvez, M.D., Potin, P., Haras, D., and Bazire, A. (2012)
- 530 Influence of Exudates of the Kelp *Laminaria Digitata* on Biofilm Formation of Associated and
- 531 Exogenous Bacterial Epiphytes. *Microbial Ecology* **64**: 359–369.
- 532 Schloss, P.D., Jenior, M.L., Koumpouras, C.C., Westcott, S.L., and Highlander, S.K. (2016)
- 533 Sequencing 16S rRNA gene fragments using the PacBio SMRT DNA sequencing system. *PeerJ*
- 534 **4**: e1869.
- 535 Schloss, P.D., Westcott, S.L., Ryabin, T., Hall, J.R., Hartmann, M., Hollister, E.B., et al.
- 536 (2009) Introducing mothur: open-source, platform-independent, community-supported software
- 537 for describing and comparing microbial communities. *Applied and environmental microbiology*
- 538 **75**: 7537–7541.

539 Tarquinio, F., Hyndes, G.A., Laverock, B., Koenders, A., and Säwström, C. (2019) The  
540 seagrass holobiont: Understanding seagrass-bacteria interactions and their role in seagrass  
541 ecosystem functioning. *FEMS Microbiology Letters* **366**:

542 Tujula, N.A., Crocetti, G.R., Burke, C., Thomas, T., Holmström, C., and Kjelleberg, S. (2010)  
543 Variability and abundance of the epiphytic bacterial community associated with a green marine  
544 Ulvacean alga. *The ISME Journal* **4**: 301–311.

545 Ugarelli, K., Laas, P., and Stingl, U. (2019) The microbial communities of leaves and roots  
546 associated with turtle grass (*Thalassia testudinum*) and manatee grass (*syringodium filliforme*) are  
547 distinct from seawater and sediment communities, but are similar between species and sampling  
548 sites. *Microorganisms* **7**:

549 Uku, J., Björk, M., Bergman, B., and Díez, B. (2007) Characterization and comparison of  
550 prokaryotic epiphytes associated with three East African seagrasses. *Journal of Phycology* **43**:  
551 768–779.

552 Weidner, Arnold, Stackebrandt, and Pühler (2000) Phylogenetic Analysis of Bacterial  
553 Communities Associated with Leaves of the Seagrass *Halophila stipulacea* by a Culture-Independent  
554 Small-Subunit rRNA Gene Approach. *Microbial ecology* **39**: 22–31.

555 Wickham, H., Averick, M., Bryan, J., Chang, W., McGowan, L.D., François, R., et al. (2019)  
556 Welcome to the tidyverse. *Journal of Open Source Software* **4**: 1686.

557 Xie, Y. (2015) Dynamic Documents with {R} and knitr, 2nd ed. Boca Raton, Florida:  
558 Chapman; Hall/CRC.

559 Xie, Y. (2014) knitr: A Comprehensive Tool for Reproducible Research in {R}. In,  
560 Stodden, V., Leisch, F., and Peng, R.D. (eds), *Implementing reproducible computational research*.  
561 Chapman; Hall/CRC.

562 Xie, Y. (2019a) knitr: A General-Purpose Package for Dynamic Report Generation in R.

563 Xie, Y. (2019b) TinyTeX: A lightweight, cross-platform, and easy-to-maintain LaTeX  
564 distribution based on TeX Live. *TUGboat* 30–32.

565 Xie, Y. (2020) tinytex: Helper Functions to Install and Maintain 'TeX Live', and Compile  
566 'LaTeX' Documents.

567 Xie, Y., Allaire, J.J., and Grolemund, G. (2018) R Markdown: The Definitive Guide, Boca  
568 Raton, Florida: Chapman; Hall/CRC.

569 Xie, Z., Lin, W., and Luo, J. (2017) Comparative Phenotype and Genome Analysis of  
570 *Cellvibrio* sp. PR1, a Xylanolytic and Agarolytic Bacterium from the Pearl River. *BioMed*  
571 *research international* **2017**: 6304248.

572 Yilmaz, P., Parfrey, L.W., Yarza, P., Gerken, J., Pruesse, E., Quast, C., et al. (2014) The SILVA  
573 and "All-species Living Tree Project (LTP)" taxonomic frameworks. *Nucleic acids research* **42**:  
574 D643–8.

575 Zavodnik, N., Travizi, A., and De Rosa, S. (1998) Seasonal variations in the rate of  
576 pliotosynthetic activity and chemical composition of the seagrass *Cymodocea nodosa* (Ucr.) Asch.  
577 *Scientia Marina* **62**: 301–309.

578 Zhu, H. (2019) kableExtra: Construct Complex Table with 'kable' and Pipe Syntax.

579 **Figure Captions**

580 **Figure 1.** Proportion of shared bacterial and archaeal OTUs (Jaccard's Similarity Coefficient)  
581 and shared bacterial and archaeal communities (Bray-Curtis Similarity Coefficient) between  
582 communities associated with the surfaces of macrophytes (*C. nodosa* [Invaded] and *C. cylindracea*  
583 [Invaded and Noninvaded]) and coomunities in the ambient seawater.

584 **Figure 2.** Proportion of shared bacterial and archaeal communities (Bray-Curtis Similarity  
585 Coefficient) and shared bacterial and archaeal OTUs (Jaccard's Similarity Coefficient) between  
586 consecutive sampling points and from the surfaces of macrophytes (*C. nodosa* [Invaded] and *C.*  
587 *cylindracea* [Invaded and Noninvaded]) and in the ambient seawater.

588 **Figure 3.** Principal Coordinates Analysis (PCoA) of Bray-Curtis distances based on OTU  
589 abundances of bacterial and archaeal communities from the surfaces of macrophytes (*C. nodosa*  
590 [Invaded] and *C. cylindracea* [Invaded and Noninvaded]) and in the ambient seawater. Samples  
591 from the same environment or same season are labeld in different colors. The proportion of  
592 explained variation by each axis is shown on the corresponding axis in parentheses.

593 **Figure 4.** Taxonomic classification and relative contribution of the most abundant (> 1 %) bacterial  
594 and archaeal sequences on the surfaces of macrophytes (*C. nodosa* [Invaded] and *C. cylindracea*  
595 [Invaded and Noninvaded]) and in the ambient seawater.

596 **Figure 5.** Taxonomic classification and relative contribution of the most abundant (> 1 %)  
597 cyanobacterial sequences on the surfaces of macrophytes (*C. nodosa* [Invaded] and *C. cylindracea*  
598 [Invaded and Noninvaded]) and in the ambient seawater. The proportion of cyanobacterial  
599 sequences in the total bacterial and archaeal community is given above the corresponding bar. NR  
600 – No Relative

601 **Figure 6.** Taxonomic classification and relative contribution of the most abundant (> 2 %)  
602 sequences within the *Bacteroidota* on the surfaces of macrophytes (*C. nodosa* [Invaded] and *C.*

603 *cylindracea* [Invaded and Noninvaded]) and in the ambient seawater. The proportion of sequences  
604 classified as *Bacteroidota* in the total bacterial and archaeal community is given above the  
605 corresponding bar. NR – No Relative

606 **Figure 7.** Taxonomic classification and relative contribution of the most abundant (> 2 %)  
607 alphaproteobacterial sequences on the surfaces of macrophytes (*C. nodosa* [Invaded] and  
608 *C. cylindracea* [Invaded and Noninvaded]) and in the ambient seawater. The proportion of  
609 alphaproteobacterial sequences in the total bacterial and archaeal community is given above the  
610 corresponding bar. NR – No Relative

611 **Figure 8.** Taxonomic classification and relative contribution of the most abundant (> 2 %)  
612 gammaproteobacterial sequences on the surfaces of macrophytes (*C. nodosa* [Invaded] and  
613 *C. cylindracea* [Invaded and Noninvaded]) and in the ambient seawater. The proportion of  
614 gammaproteobacterial sequences in the total bacterial and archaeal community is given above the  
615 corresponding bar. NR – No Relative

616 **Figure 9.** Taxonomic classification and relative contribution of the most abundant (> 1 %)  
617 sequences within the *Desulfobacterota* on the surfaces of macrophytes (*C. nodosa* [Invaded]  
618 and *C. cylindracea* [Invaded and Noninvaded]) and in the ambient seawater. The proportion of  
619 sequences classified as *Desulfobacterota* in the total bacterial and archaeal community is given  
620 above the corresponding bar. NR – No Relative

621 **Figures**

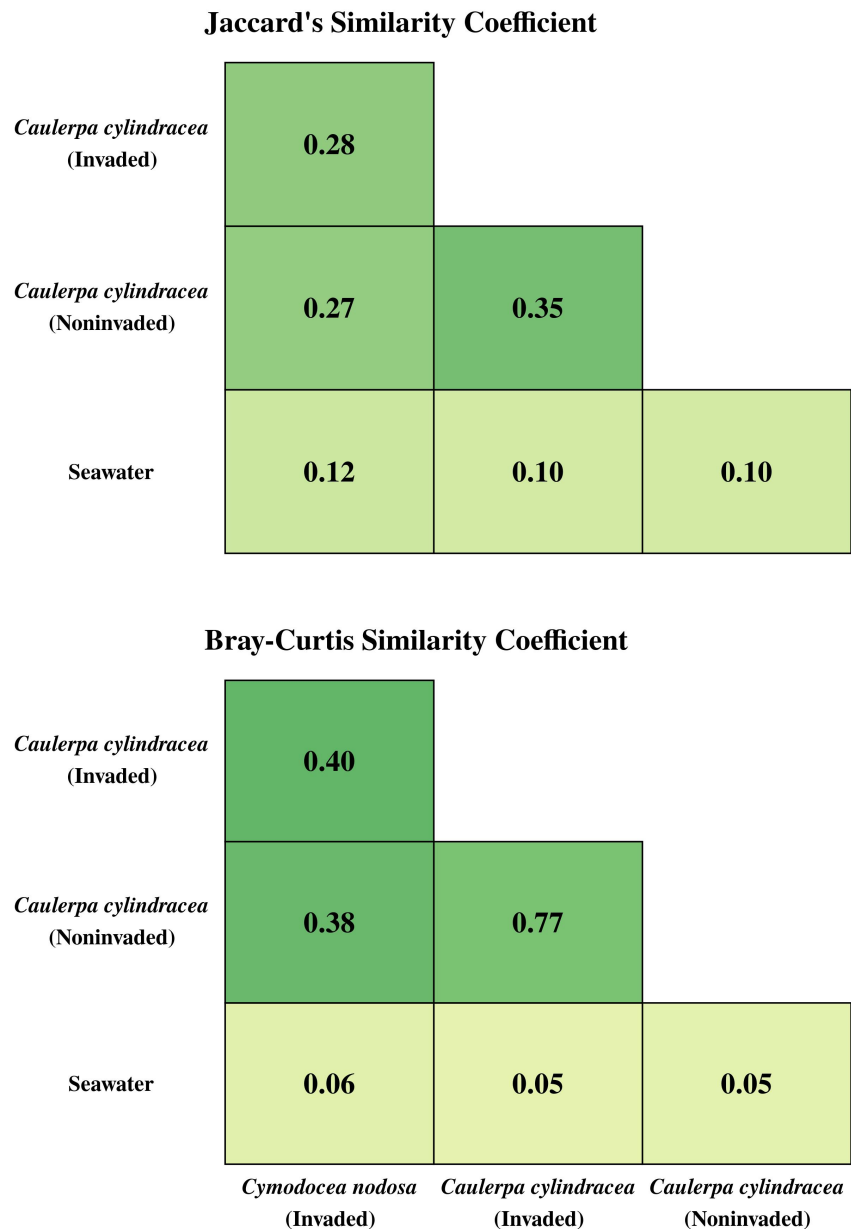


**Figure 1.** Proportion of shared bacterial and archaeal OTUs (Jaccard's Similarity Coefficient) and shared bacterial and archaeal communities (Bray-Curtis Similarity Coefficient) between communities associated with the surfaces of macrophytes (*C. nodosa* [Invaded] and *C. cylindracea* [Invaded and Noninvaded]) and coomunities in the ambient seawater.

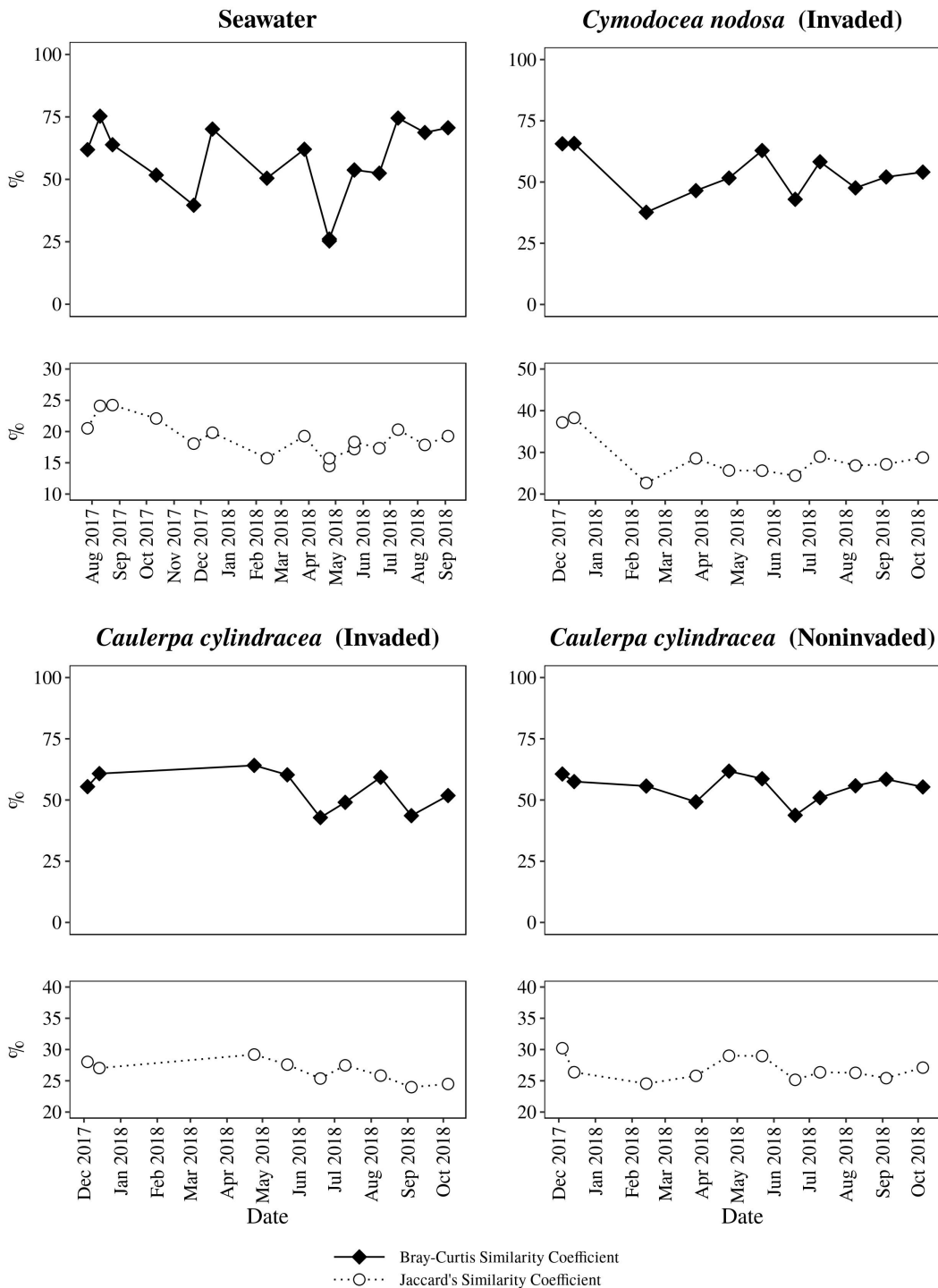


**Figure 2.** Proportion of shared bacterial and archaeal communities (Bray-Curtis Similarity Coefficient) and shared bacterial and archaeal OTUs (Jaccard's Similarity Coefficient) between consecutive sampling points and from the surfaces of macrophytes (*C. nodosa* [Invaded] and *C. cylindracea* [Invaded and Noninvaded]) and in the ambient seawater.

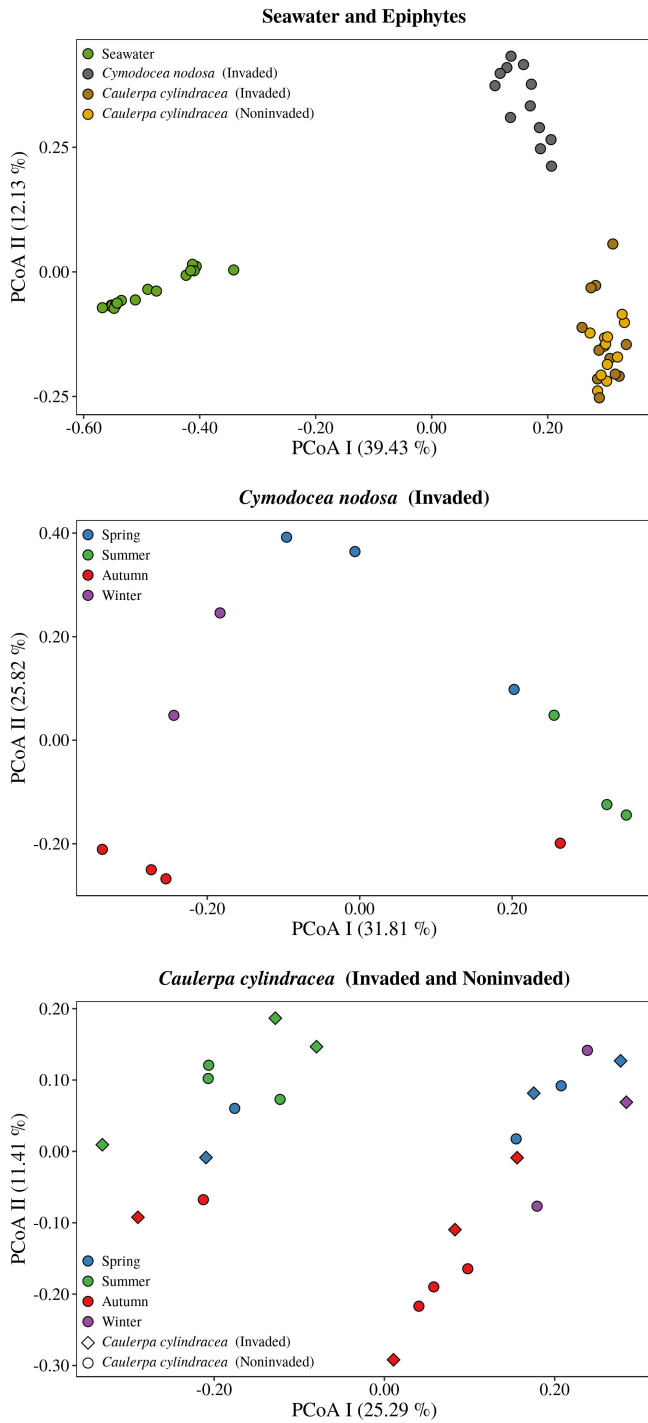


**Figure 3.** Principal Coordinates Analysis (PCoA) of Bray-Curtis distances based on OTU abundances of bacterial and archaeal communities from the surfaces of macrophytes (*C. nodosa* [Invaded] and *C. cylindracea* [Invaded and Noninvaded]) and in the ambient seawater. Samples from the same environment or same season are labeled in different colors. The proportion of explained variation by each axis is shown on the corresponding axis in parentheses.

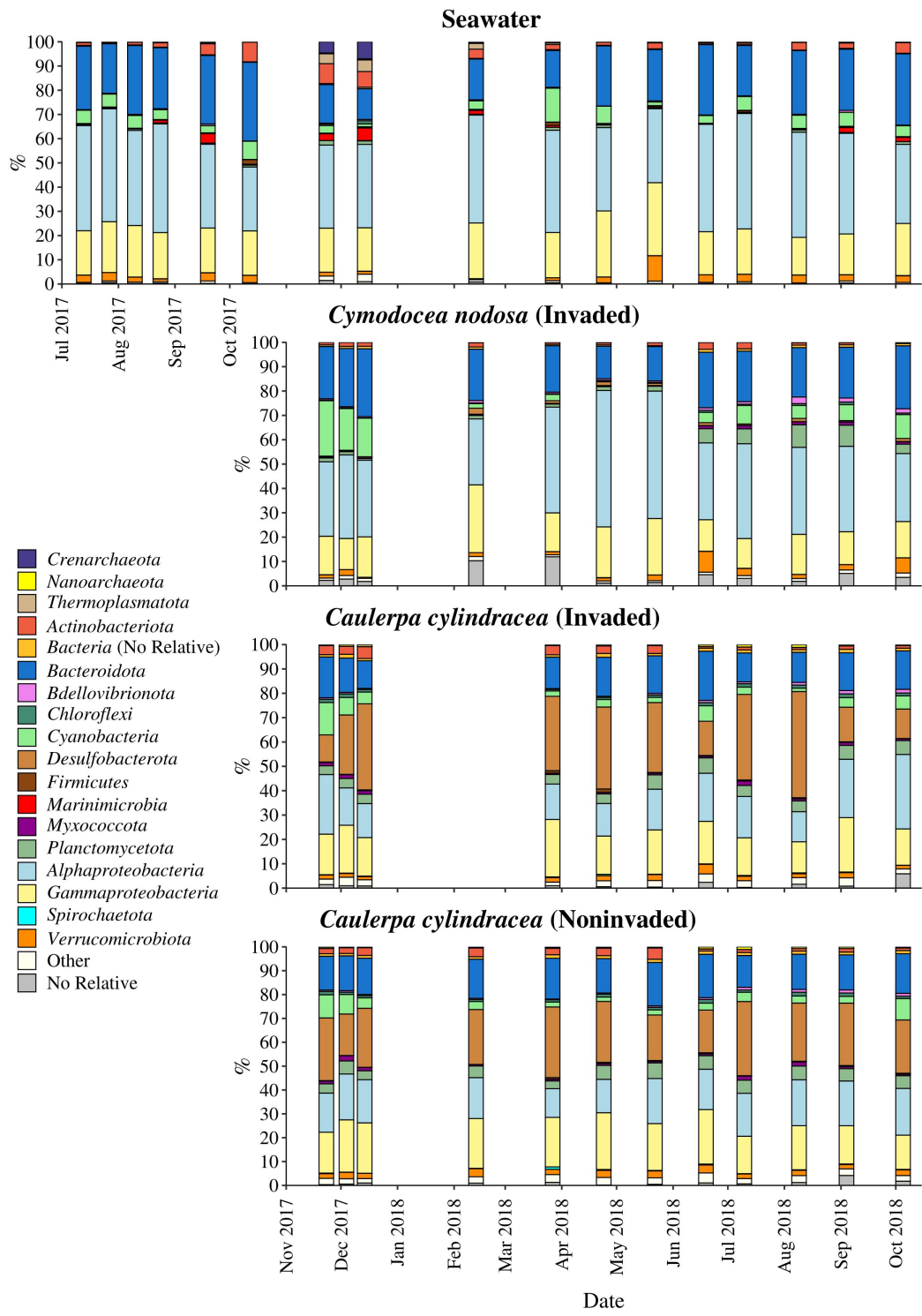


**Figure 4.** Taxonomic classification and relative contribution of the most abundant (> 1 %) bacterial and archaeal sequences on the surfaces of macrophytes (*C. nodosa* [Invaded] and *C. cylindracea* [Invaded and Noninvaded]) and in the ambient seawater.

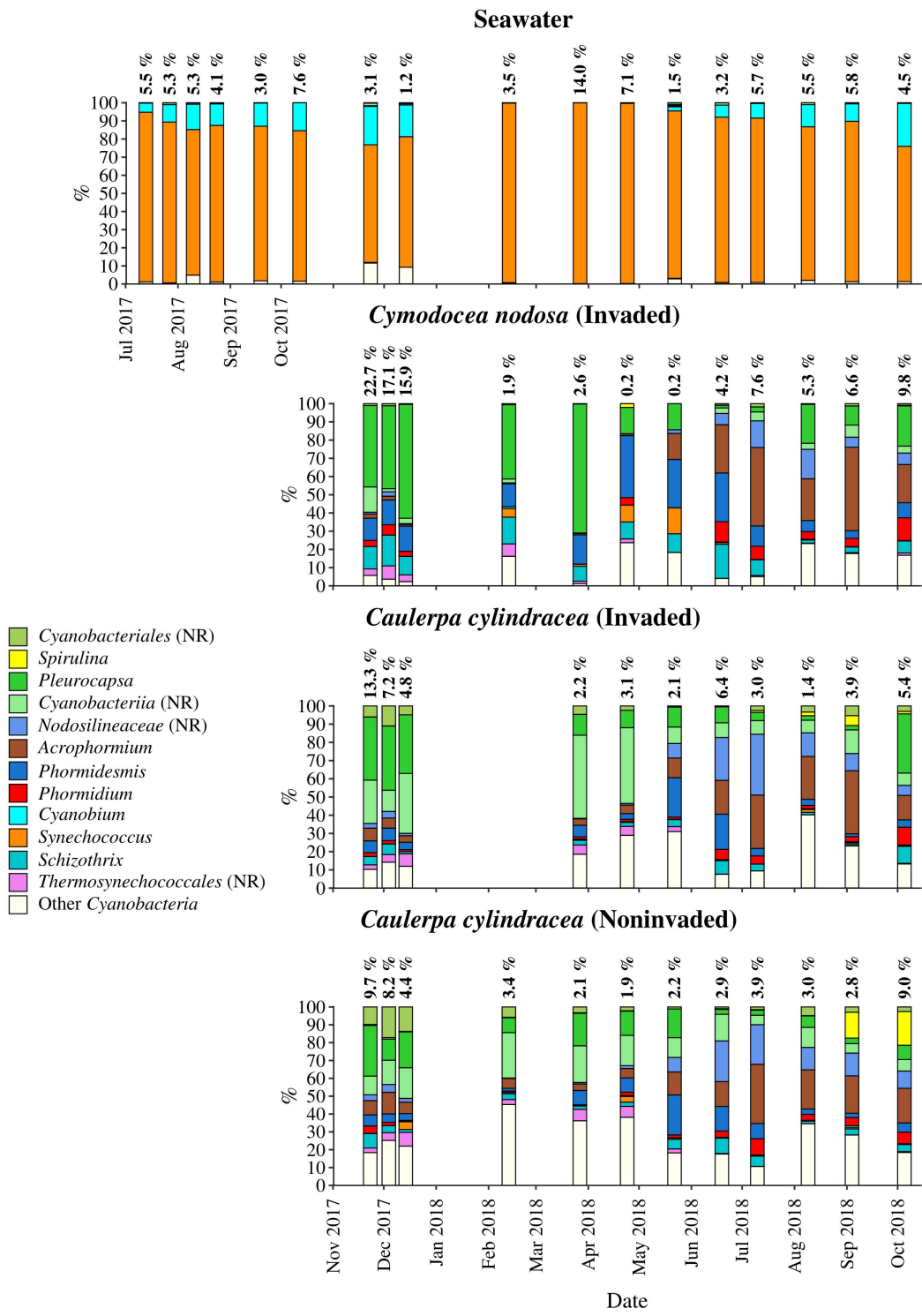


**Figure 5.** Taxonomic classification and relative contribution of the most abundant (> 1 %) cyanobacterial sequences on the surfaces of macrophytes (*C. nodosa* [Invaded] and *C. cylindracea* [Invaded and Noninvaded]) and in the ambient seawater. The proportion of cyanobacterial sequences in the total bacterial and archaeal community is given above the corresponding bar. NR – No Relative

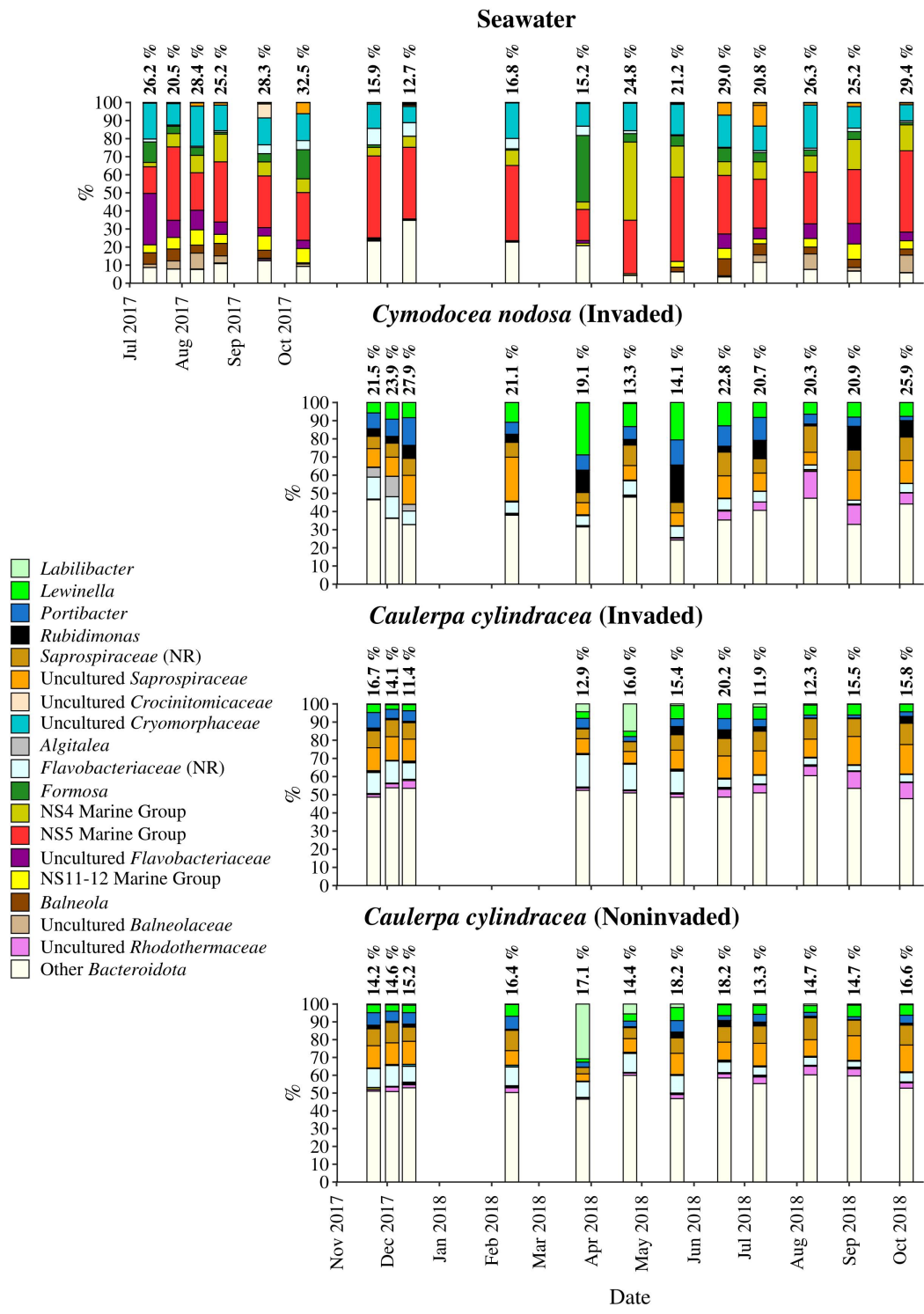


**Figure 6.** Taxonomic classification and relative contribution of the most abundant (> 2 %) sequences within the *Bacteroidota* on the surfaces of macrophytes (*C. nodosa* [Invaded] and *C. cylindracea* [Invaded and Noninvaded]) and in the ambient seawater. The proportion of sequences classified as *Bacteroidota* in the total bacterial and archaeal community is given above the corresponding bar. NR – No Relative

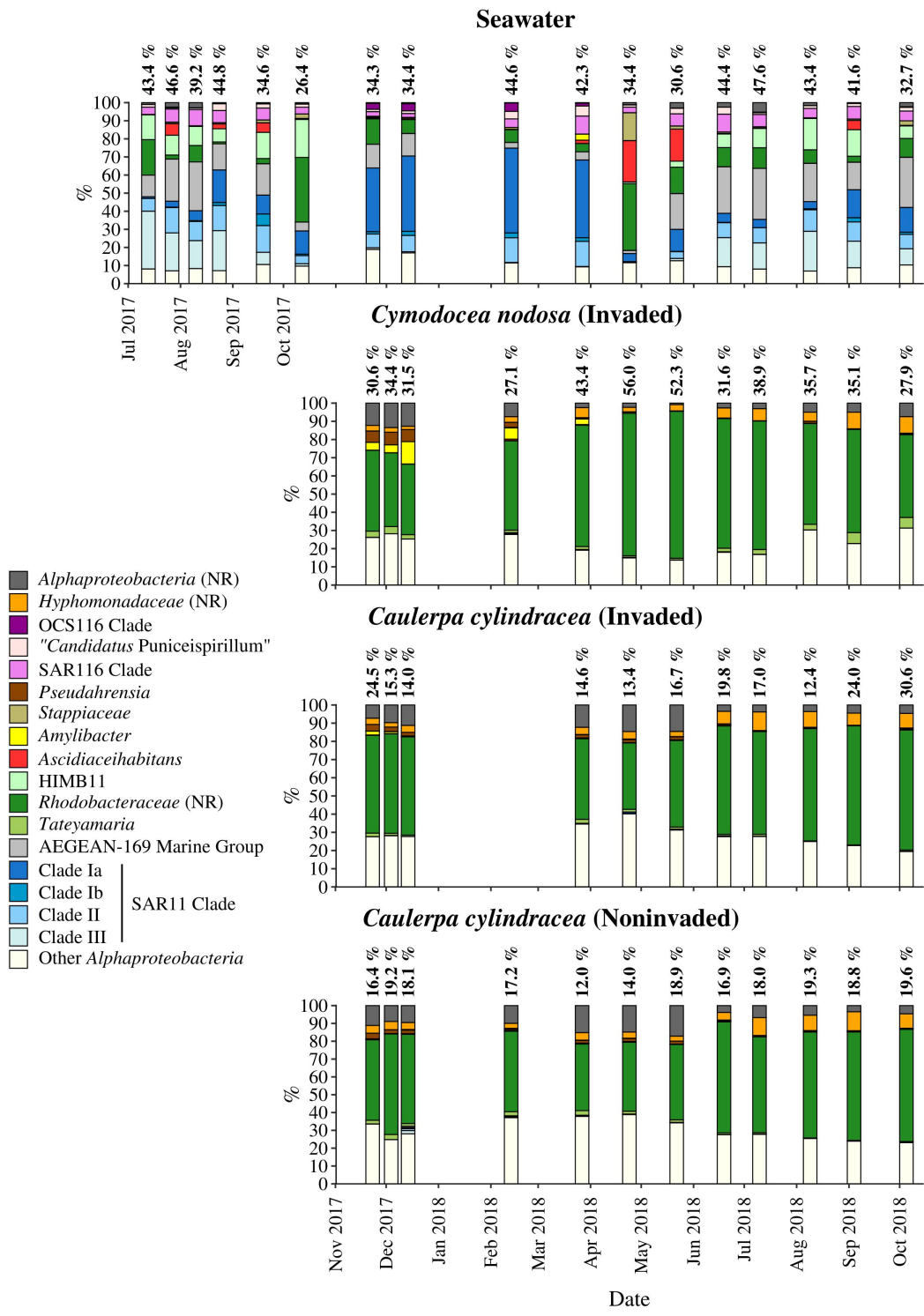


**Figure 7.** Taxonomic classification and relative contribution of the most abundant (> 2 %) alphaproteobacterial sequences on the surfaces of macrophytes (*C. nodosa* [Invaded] and *C. cylindracea* [Invaded and Noninvaded]) and in the ambient seawater. The proportion of alphaproteobacterial sequences in the total bacterial and archaeal community is given above the corresponding bar. NR – No Relative

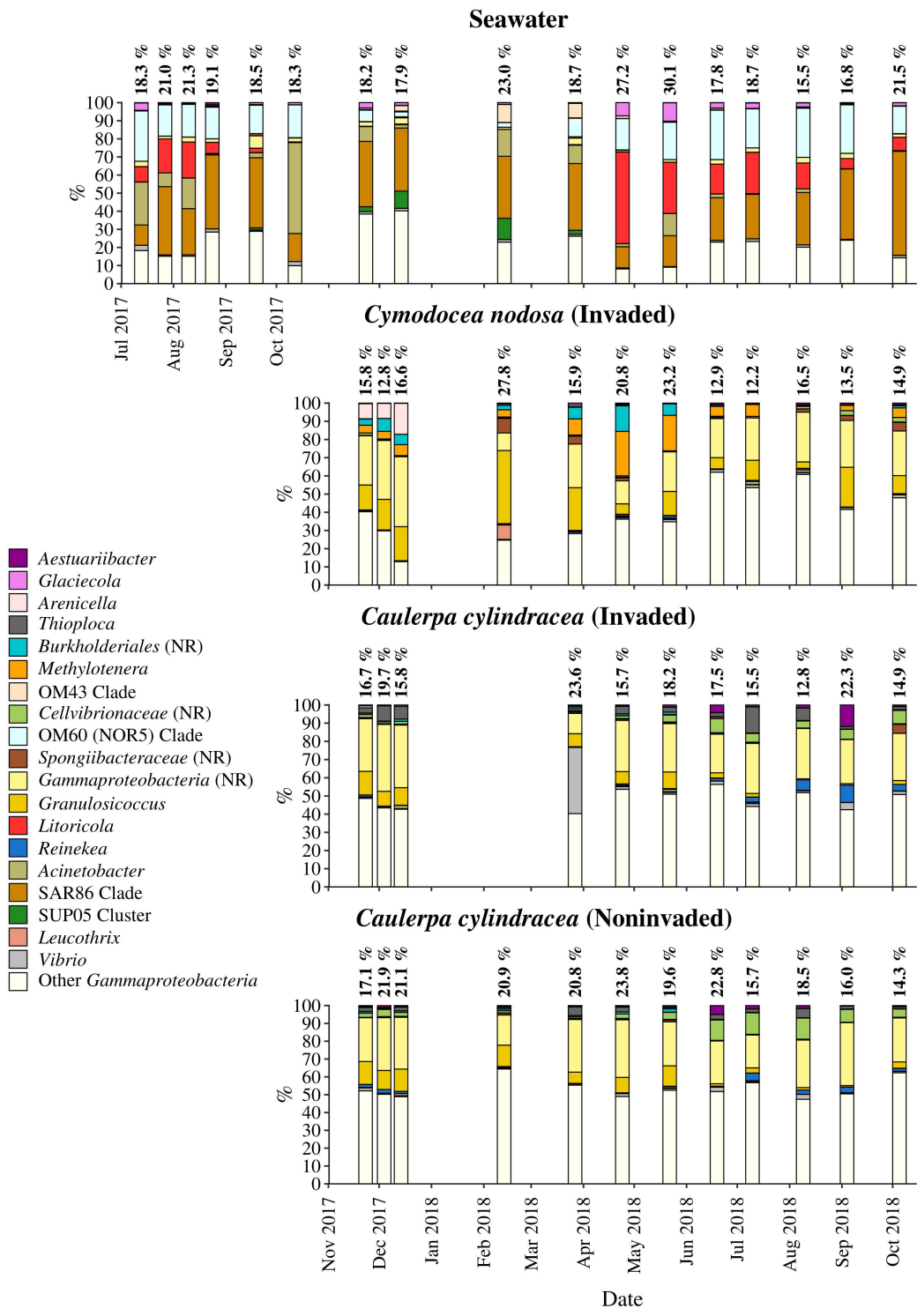


**Figure 8.** Taxonomic classification and relative contribution of the most abundant (> 2 %) gammaproteobacterial sequences on the surfaces of macrophytes (*C. nodosa* [Invaded] and *C. cylindracea* [Invaded and Noninvaded]) and in the ambient seawater. The proportion of gammaproteobacterial sequences in the total bacterial and archaeal community is given above the corresponding bar. NR – No Relative

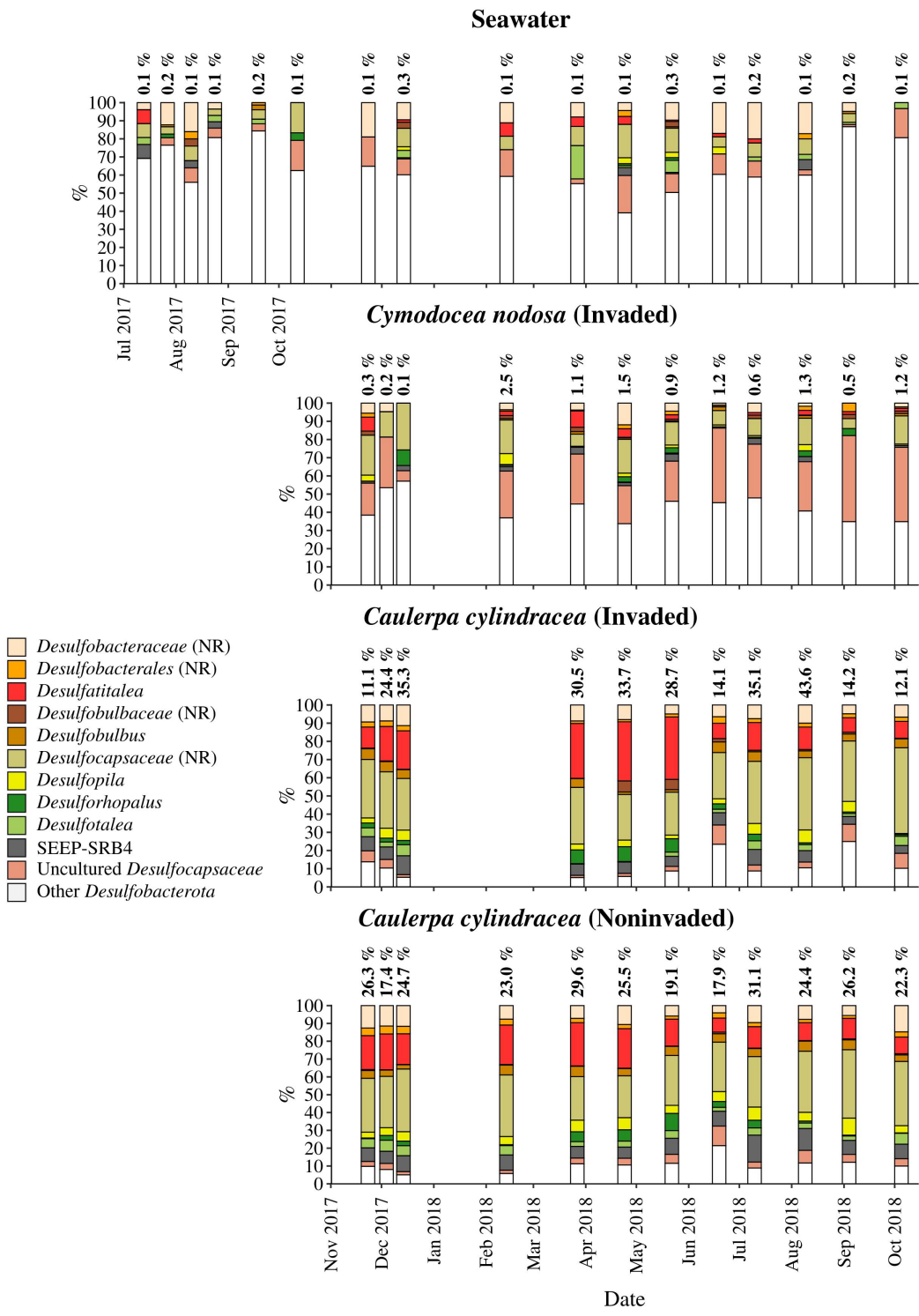


**Figure 9.** Taxonomic classification and relative contribution of the most abundant (> 1 %) sequences within the *Desulfobacterota* on the surfaces of macrophytes (*C. nodosa* [Invaded] and *C. cylindracea* [Invaded and Noninvaded]) and in the ambient seawater. The proportion of sequences classified as *Desulfobacterota* in the total bacterial and archaeal community is given above the corresponding bar. NR – No Relative